Crystal nucleation in undercooled liquid zirconium

Stefan Klein,* Dirk Holland-Moritz, and Dieter M. Herlach†
Institut für Materialphysik im Weltraum, Deutsches Zentrum für Luft- und Raumfahrt, 51170 Köln, Germany
(Received 2 June 2009; revised manuscript received 2 September 2009; published 10 December 2009)

Electromagnetic and electrostatic levitation are applied to undercool melts of pure Zr. Each sample is undercooled approximately 100 times and the distribution functions of undercoolings are determined. They are analyzed within a statistical approach of classical nucleation theory. Despite large undercoolings the analysis predicts heterogeneous nucleation in electromagnetic levitation. Electrostatic levitation leads to an increase of average undercooling and the statistical analysis indicates that the undercoolings approach the limit as given by homogeneous nucleation.

DOI: 10.1103/PhysRevB.80.212202 PACS number(s): 64.60.Q−, 64.70.kd, 64.70.mj

Crystallization of liquids is a first-order phase transition and initiated by nucleation. The activation barrier of nucleation controls the undercooling level measured in experiments. One distinguishes between heterogeneous nucleation and homogeneous nucleation. Heterogeneous nucleation is an *extrinsic* process in which container walls and/or foreign phases in the melt participate in. In contrast homogeneous nucleation is an *intrinsic* process, in which the undercooled liquid and the solid nucleus are involved. Hence, heterogeneous nucleation is governed by the experimental conditions whereas homogeneous nucleation depends on the properties of the system investigated.

In the present work we apply electromagnetic (EML) and electrostatic levitation (ESL) techniques to investigate the maximum undercooling of pure Zr. Using these containerless processing methods heterogeneous nucleation on container walls is completely circumvented. Samples were processed by about 100 heating and cooling cycles in both experimental setups. The probability distribution of undercoolings measured in both levitators are analyzed within a model of Skripov.[1] The evaluation of the undercooling distribution functions yields the activation energy of crystal nucleation and the density of nucleation sites. Both quantities were found to be different for EML and ESL experiments. The results are discussed with respect to the physical nature of nucleation observed in both different sets of experiments.

Sphere like Zirconium samples were prepared from ingot material purchased from Teledyne Wah Chang with a purity of 99.995% cut into pieces and melted in an arc furnace made of UHV compatible stainless steel components under high purity Ar gas (6N). For EML (Ref. 2) the samples of 8 mm in diameter are processed in an ultrahigh vacuum chamber, which is evacuated to a pressure of 10^{-7} mbar before backfilling with He gas with a purity of 6N. The compensation of the gravitational force implies a minimum power absorption to levitate the sample. Heat radiation is not sufficient to transfer the heat produced in the electromagnetically levitated sample and to cool it below its melting temperature. Therefore, cooling by forced convection with He of high purity is used to cool the sample. For ESL,[3] samples of 2 mm in diameter are processed under ultra high vacuum conditions ($\approx 2\times 10^{-8}$ mbar). Levitation and heating is decoupled in contrast to EML. In both levitation setups the temperature is measured by a pyrometer with an absolute accuracy of ± 5 K and a relative accuracy of ± 1 K.

Figure 1 shows a temperature-time profile measured on a Zr sample processed in the ESL (cf. inset). First, the solid sample is heated up to its melting temperature, T_m. In case of a pure metal as Zr the sample melts congruently at T_m. The small step in the melting plateau is due to the change in spectral emissivity when the solid transforms to the liquid. After complete melting the liquid sample is heated to a temperature well above T_m before cooling. Since heterogeneous nucleation at container walls and impurity sites are significantly reduced, the liquid sample undercools well below T_m. When spontaneous nucleation sets in at an undercooling $\Delta T = T_m - T_n$ (T_n: nucleation temperature) the nucleated crystal rapidly grows due to a large thermodynamic driving force generated at such deep undercoolings. The rapid release of the heat of crystallization leads to a steep rise of temperature called recalescence. From such temperature-time profiles ΔT is easily inferred since T_n is well defined by the onset of recalescence. After the entire sample has solidified the next heating and cooling cycle is started.

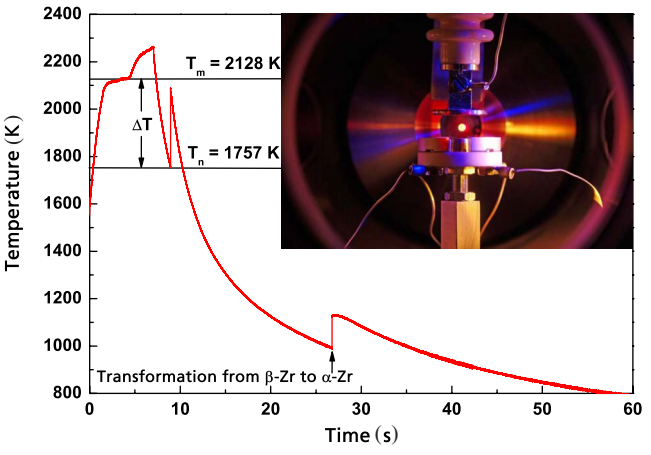

FIG. 1. (Color online) Temperature-time profile measured by a pyrometer on a zirconium drop levitated in an electrostatic levitator under ultra high vacuum. The melting plateau at $T_m = 2128$ K is obvious. At $T_n = 1757$ K spontaneous nucleation sets in and the subsequent rapid crystal growth of β-Zr solid phase (bcc) leads to a steep rise of temperature during recalescence. The second recalescence event at 980 K is attributed to a structural phase transformation of solid β-Zr to solid α-Zr phase (hcp). The inset shows an electrostatically levitated Zr drop.

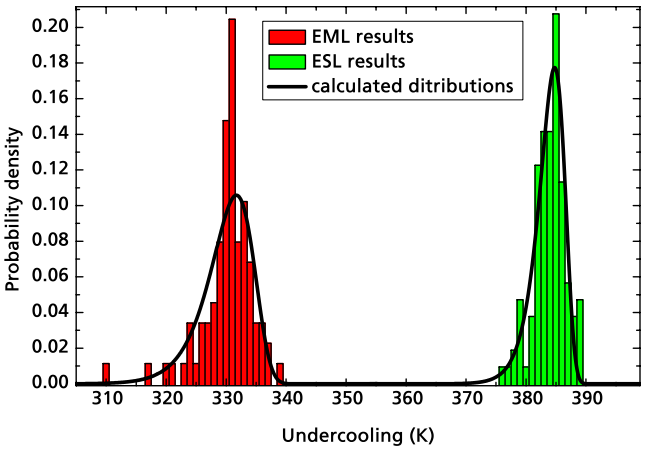

FIG. 2. (Color online) Probability distribution functions of undercoolings measured in 100 experiment cycles on pure Zr in the electromagnetic (left) and the electrostatic levitator (right). The solid lines give the probability distribution function as computed according to a statistical analysis of nucleation undercooling.

Usually, the solidification of an undercooled metallic melt is a two-staged process. During recalescence a fraction of the sample, f_R, solidifies under nonequilibrium condition and during post recalescence the remaining melt, $f_{pr}=1-f_R$, solidifies under near-equilibrium conditions. f_R increases with the degree of undercooling and becomes unity, $f_R=1$ if $\Delta T=\Delta T_{hyp}$. The hypercooling limit, ΔT_{hyp}, is reached if the heat of fusion ΔH_f is just sufficient to heat the sample with its specific heat C_p up to T_m. In case of quasiadiabatic conditions, i.e., if the amount of heat transferred to the environment is negligible compared to the heat produced during recalescence, the hypercooling limit is given by $\Delta T_{hyp}=\frac{\Delta H_f}{C_p}$. In case of pure Zr the hypercooling limit is estimated as $\Delta T_{hyp}=359$ K with $\Delta H_f=14652$ J/mol and $C_p=40.8$ J mol/K.[4] With increasing undercooling, $\Delta T>\Delta T_{hyp}$, the post-recalescence plateau vanishes and T_m will not be reached during recalescence. As can be seen from Fig. 1, in this experiment an undercooling of $\Delta T=371$ K is measured, which is larger than ΔT_{hyp}. Hypercooling was also reported for Co-Pd alloys.[5]

Figure 2 shows the distribution functions of undercoolings measured in the electromagnetic levitator (left) and the electrostatic levitator (right). To analyze the experimental results we refer to a statistical model developed by Skripov.[1] It has been previously applied to investigate nucleation behavior in Co-Pd alloys (with high magnetic Curie temperatures).[6] According to nucleation theory[7] the activation energy ΔG^* for the formation of a nucleus of critical size is given by

$$\Delta G^* = \frac{16}{3}\pi\frac{\sigma^3}{\Delta G_V^2}\cdot f(\vartheta), \tag{1}$$

with σ the solid-liquid interfacial energy, $\Delta G_V=G_L-G_S$ the difference of Gibbs free energy per unit volume of liquid (G_L) and solid (G_S) phase, and $f(\vartheta)$ the catalytic potency factor for heterogeneous nucleation. In case of homogeneous nucleation $f(\vartheta)=1$. For pure metals the driving force for nucleation ΔG_V can be approximated by $\Delta G_V=\Delta S_f\cdot\Delta T\cdot V_m^{-1}$ with $\Delta S_f=\Delta H_f/T_m$ and ΔH_f the enthalpy of fusion and V_m the molar volume.[8] The solid-liquid interfacial energy σ is given by the negentropic model[9] as

$$\sigma = \alpha\cdot\frac{\Delta S_f\cdot T}{(N_A V_m^2)^{1/3}}, \tag{2}$$

with N_A Avogadro's number and $\alpha=0.70$ for bcc structured solid β-Zr that primarily nucleates in the undercooled melt. The steady state nucleation rate, I_{ss}, is computed as[10]

$$I_{ss} = K_V\cdot\exp\left(-\frac{\Delta G^*}{k_B T}\right) = K_V\cdot\exp\left(-\frac{CT^2}{\Delta T^2}\right), \tag{3}$$

with

$$K_V = \frac{k_B T N_0}{3a_0^3\eta(T)};\quad C = \frac{16\pi\Delta S_f\alpha^3 f(\vartheta)}{3k_B N_A}, \tag{4}$$

where $\eta(T)$ denotes the temperature dependent viscosity, a_o a typical interatomic spacing, k_B Boltzmann's constant and N_0 the number of potential nucleation sites. For homogeneous nucleation, K_V in Eq. (4) is in the order of magnitude of $K_V\approx 10^{+39}$ m^{-3} s^{-1},[10] because each atom in the melt can act as a potential nucleation site, $N_0=N_A/V_m$. In case of heterogeneous nucleation, only atoms at the catalyzing substrate can act as a nucleation site. Therefore N_0 and hence K_V is drastically reduced as compared with homogeneous nucleation.

Nucleation is a stochastic process of rare and independent events. Therefore, the Poisson distribution is applied to determine K_V and C of Eq. (3) from the distribution function of the measured undercoolings.[1] Under nonisothermal conditions (cooling rate $\dot{T}\neq 0$) the probability ω for one nucleation event in a sample of volume V ($N_n=N_0V$) within the temperature interval T and $T+\delta T$ is given by

$$\omega(1,T+\delta T) = \delta T\frac{VI_{ss}(T)}{|\dot{T}|}\cdot\exp\left[-\int_{T_m}^{T}\frac{VI_{ss}(T)}{\dot{T}}dT\right]. \tag{5}$$

From Eq. (3)–(5) the cumulative distribution function $F(T)$ is determined[7]

$$F(T) = 1-\exp\left[-\frac{V}{\dot{T}}\int_{T_m}^{T}K_V\cdot\exp\left(\frac{CT^2}{\Delta T^2}\right)dT\right]. \tag{6}$$

In the present investigations the temperatures are close to T_m. These temperatures are far away from the glass transition temperature $T_g\approx 0.3\cdot T_m$ of pure metals. Therefore, the temperature dependence of the exponential function containing the activation energy $\Delta G^*(T)$ is much more dominant compared to that of the prefactor of the nucleation rate that is depending on viscosity $\eta(T)$. The temperature dependence of $\eta(T)$ is weak close to T_m but steeply rises if T is approaching T_g. If the temperature dependence of the prefactor K_V is neglected, Eqs. (5) and (6) are simplified as[7]

TABLE I. $\overline{\Delta T}=\Delta T_m-T_n$: average undercooling, $\overline{\Delta T_r}=\overline{\Delta T}/T_m$: relative undercooling, W: half width of the distribution function, b and C: parameters as inferred from the nucleation analysis, K_V: pre-exponential factor of the nucleation rate according to Eq. (4).

	$\overline{\Delta T}$ (K)	$\overline{\Delta T_r}$ (K)	W	b	$-C$	K_V [m^{-3} s^{-1}]	ΔG^*
ESL	384	0.180	5.1	73.95	3.51	10^{+42}	$75\cdot k_BT$
EML	330	0.155	8.5	47.58	1.62	10^{+25}	$42\cdot k_BT$
ESL[a]	348	0.16				10^{+43}	$88\cdot k_BT$

[a]Ref. 12.

$$F(T)=1-\exp\left[-\frac{VK_V}{\dot{T}d\left(-\frac{\Delta G^*}{k_BT}\right)/dT}\cdot\exp\left(\frac{CT^2}{\Delta T^2}\right)dT\right], \quad (7)$$

According to Eq. (7) a plot of $\ln[-\ln(1-F(T)\ ]$ vs. $T^2/\Delta T^2$ gives a linear relation from which the slope C, and the intercept b are inferred

$$b=\ln\left[\frac{VK_V}{\dot{T}d\left(-\frac{\Delta G^*}{k_BT}\right)/dT}\right], \quad (8)$$

with

$$\frac{d\left(-\frac{\Delta G^*}{k_BT}\right)}{dT}=2C\frac{T\cdot\Delta T+T^2}{\Delta T^3}, \quad (9)$$

K_V and $\alpha\cdot f(\vartheta)^{1/3}$ are deduced from C and b. The average relative undercoolings, $\overline{\Delta T}/T_m$, the half widths of the distribution functions W, the parameters C and b as inferred from the nucleation undercooling analysis, the prefactors K_V and the activation energies ΔG^* are compiled in Table I.

The functions $\omega(1,T+\delta T)$ are plotted in Fig. 2 (solid lines) together with the experimentally determined distribution functions of measured undercoolings (bars). Both, the average undercooling and the half-width of the distribution functions obviously differ for both sets of experiments performed with EML and ESL. With ESL an average undercooling of about $\overline{\Delta T}_{ESL}=384$ K is observed which is significantly higher than the average undercooling as measured by EML, $\overline{\Delta T}_{EML}=330$ K. The half width of the distribution function measured by EML is broader compared to the results obtained from measurements by ESL. The distribution function as measured in the ESL shows a steep drop on the high undercooling-region indicating the onset of homogeneous nucleation. In case of homogeneous nucleation the distribution function of undercooling falls much steeper on the high undercooling side as compared with the case of heterogeneous nucleation.[11]

For a direct comparison of both sets of investigations the as determined mean undercoolings have to be normalized in order to take into account the different size of the samples and the different cooling rates of the experiments. Assuming that one nucleation event is sufficient to initialize solidification of the undercooled melt, the following equation holds

$$\int_0^t I_{ss}\cdot V dt'=1. \quad (10)$$

The integral is taken over the experimental time t. t can be approximated by $t=\Delta T/\dot{T}$ with $\dot{T}$ the cooling rate and ΔT the undercooling as inferred from the measured temperature-time profiles.

As soon as one nucleation event takes place solidification is completed by subsequent rapid dendrite growth.[7] From the measurements of the temperature-time profiles we infer cooling rates of $\dot{T}_{EML}=\Delta T/\Delta t\approx 25$ K/s and $\dot{T}_{ESL}\approx 250$ K/s, respectively. Using the nucleation rate function determined from the Skripov analysis with Eq. (10) the mean undercooling can be calculated which an EML experiment would deliver at same cooling rates and sample size as in the ESL experiment. This gives a converted mean undercooling of 352 K which is still 32 K smaller than that observed in the ESL experiment. This is a consequence of activation energy ΔG^* and prefactor K_V as determined in the framework of the Skripov model for the levitation experiments.

The activation energy $\Delta G^*_{ESL}=75\ k_BT$ for the formation of a critical sized nucleus as determined from the ESL experiment is by about a factor of 2 larger than $\Delta G^*_{EML}=42\ k_BT$ determined from the result of the EML experiments. The prefactor K_V also differs essentially for both sets of experiments. In case of the ESL experiments, $K_V^{ESL}\approx 10^{+42}$ m^{-3} s^{-1} which is much higher than $K_V^{EML}\approx 10^{+25}$ m^{-3} s^{-1}. The main differences between both sets of experiments are the environmental conditions such that the sample is electromagnetically levitated in an He atmosphere in purity of 6 N. At a He gas pressure of 1 bar this corresponds to a pressure of impurities in the He gas of 10^{-3} mbar. This is by about five orders of magnitude higher than the residual pressure in the chamber of the ESL. In addition, the evaporation of atoms under vacuum conditions may lead to a purification of the samples and thus reduces the probability of heterogeneous nucleation on sample surface.

Hofmeister *et al.*[12] have found influence of oxygen content on the undercoolability of Zr. Interestingly, the previous results by Hofmeister *et al.* of Zr in ESL experiments show a maximum undercooling that is larger than our results obtained from EML experiments, but smaller than our results from ESL experiments. However, the results by Hofmeister *et al.* are comparable in the order of magnitude with our ESL results (cf. Table I). We attribute this finding to the fact that

the purity conditions in the ESL experiments by Hofmeister *et al.* are worse than in our ESL experiments. This means that undercooling in the previous ESL experiments is limited by heterogeneous nucleation.

Turnbull proposed a prefactor of $K_V \approx 10^{+39}$ m^{-3} s^{-1} for homogeneous nucleation.[10] This value compares with the result obtained by undercooling experiments in the ESL while it is much higher than the value obtained from electromagnetic levitation experiments. From these findings we conclude that crystallization of the undercooled melt processed by EML is initiated by heterogeneous nucleation. The undercoolings achieved by our ESL are in the vicinity of the limit of maximum undercooling as given by homogeneous nucleation. This conclusion is supported by the fact that the probability distribution functions of the ESL experiments steeply falls to zero at the high undercooling side, indicative for the onset of homogeneous nucleation. This allows for estimating the solid-liquid interfacial energy of the nucleus that is otherwise not accessible for experimental determination.

Equation (4) in combination with the results of the statistical analysis yields the product $\alpha \cdot f(\vartheta)^{1/3}=0.61$ for Zr from the undercooling experiments in the ESL. In the literature a great variety of dimensionless solid-liquid interfacial energies are reported from modeling work. The present work enables to evaluate the different approaches of solid-liquid interface modeling by comparing the modeling results with findings inferred from maximum undercooling of Zr in electrostatic levitation experiments. Since the prefactor K_V is comparable to the value given by Turnbull for homogeneous nucleation we conclude $f(\vartheta) \approx 1$. This leads to a lower limit of the dimensionless interfacial energy $\alpha \gtrsim 0.61$. The comparison with the modeling results shows that the negentropic model with $\alpha=0.70$,[9] gives the best agreement with the present experiment. Density-functional yields $\alpha \geq 0.46$ and $\alpha \geq 0.48$,[13] and molecular dynamics simulations yields $\alpha=0.29$, $\alpha=0.32$, and $\alpha=0.36$ (Ref. 14) depending on the potentials used for the simulations. All these values underestimate the solid-liquid interfacial energy inferred from the experiments. Only in the negentropic model by Spaepen a polytetrahedral short-range order in the interface is explicitly taken into account. Polytetrahedral short-range order in liquid metals is directly confirmed by neutron[15] and x-ray[16] diffraction on pure metallic liquids.

In summary, results of comparative undercooling experiments on pure Zr by applying EML and ESL are presented. In case of ESL, significantly larger undercoolings on pure Zr are observed. The hypercooling limit is exceeded for a pure metal. Undercooling distribution functions were determined from about 100 experiment cycles for both sets of experiments. The statistical analysis within classical nucleation theory gives numerical values for the activation energy and the prefactor of the nucleation rate equation. While the results of experiments conducted by EML indicate heterogeneous nucleation, the experiments in the ESL lead to the conclusion that the measured maximum undercooling approaches the limit of undercoolability as given by the onset of homogeneous nucleation. From these results a lower limit of the solid-liquid interfacial energy of a crystal nucleus is determined that is only in agreement with the negentropic model by Spaepen while more recent modeling work within density functional theory and molecular dynamics lead to an underestimation of the interfacial energy.

We thank I. Egry and H. Teichler for fruitful discussions. This work is financially supported by Deutsche Forschungsgemeischaft (DFG), under Grant No. HE 1601/21.

*Also at Institut für Festkörperphysik, Ruhr-Universität Bochum, 44780 Bochum, Germany.
†dieter.herlach@dlr.de

[1] V. P. Skripov, *Material Science, Crystal Growth and Materials* (North Holland, Amsterdam, 1977).
[2] D. M. Herlach, Annu. Rev. Mater. Sci. **21**, 23 (1991).
[3] T. Meister, H. Werner, G. Lohoefer, D. M. Herlach, and H. Unbehauen, Control Eng. Pract. **11**, 117 (2003).
[4] A. J. Rulison and W. K. Rhim, Rev. Sci. Instrum. **65**, 695 (1994).
[5] G. Wilde, G. P. Görler, and R. Willnecker, Appl. Phys. Lett. **69**, 2995 (1996).
[6] T. Schenk, D. Holland-Moritz, and D. M. Herlach, Europhys. Lett. **50**, 402 (2000).
[7] D. M. Herlach, P. Galenko, and D. Holland-Moritz, *Metastable Solids form Undercooled Metls* (Pergamon Materials Series, New York, 2007).
[8] D. Turnbull, J. Appl. Phys. **21**, 1022 (1950).
[9] D. R. Nelson and F. Spaepen, *Solid State Physics* (Academic, New York, 1989).
[10] D. Turnbull, Contemp. Phys. **10**, 473 (1969).
[11] U. Köster and U. Schünemann, *Rapidly Solidified Alloys* (Marcel Dekker, New York, 1993).
[12] W. H. Hofmeister, C. W. Morton, R. J. Bayuzick, A. J. Rulison, and J. L. Watkins, Acta Mater. **46**, 1903 (1998).
[13] D. W. Marr and A. P. Gast, J. Chem. Phys. **99**, 2024 (1993).
[14] D. Y. Sun, M. Asta, and J. J. Hoyt, Phys. Rev. B **69**, 174103 (2004).
[15] T. Schenk, D. Holland-Moritz, V. Simonet, R. Bellissent, and D. M. Herlach, Phys. Rev. Lett. **89**, 075507 (2002).
[16] G. W. Lee, A. K. Gangopadhyay, K. F. Kelton, R. W. Hyers, T. J. Rathz, J. R. Rogers, and D. S. Robinson, Phys. Rev. Lett. **93**, 037802 (2004).